

Determining the optical constants of read-write sliders during flying-height testing

Peter de Groot, Ara Dergevorkian, Tod Erickson, and Russell Pavlat

Flying-height testers for rigid disk drives employ a transparent glass substrate in place of the magnetic disk and use optical interferometry to measure the flight properties of the read-write slider. Because of the material phase change on reflection, the effective optical constants n and k of the slider play an important role in the measurement. We describe an instrument that determines the optical constants simultaneously with flying height, using polarization interferometry. This *in situ* analysis of n and k obviates the need for independent ellipsometry, while avoiding the problematic retract calibration characteristic of traditional flying-height test equipment. The rms uncertainty for n and k are 0.04, resulting in height uncertainties that range from 3 nm for 250-nm flying heights down to 0.5 nm at contact. We verify these results by use of a variety of experimental techniques on both laboratory samples and actual read-write sliders. © 1998 Optical Society of America

OCIS codes: 120.3180, 120.2130, 120.2830, 120.4530, 120.4640, 120.5410.

1. Introduction

A critical parameter in rigid-disk-drive design is the height or gap between the read-write slider and the magnetic medium. The flying height is below 50 nm at the present state of the art, but because the height is not easily measured directly, the exact value is difficult to determine in the assembled drive. For this reason, the data-storage industry relies on optical testers for quantifying flying height in production and in the development of new designs.¹ Optical testers employ a rotating, transparent glass substrate in place of the magnetic disk and determine the flying height by analysis of interference phenomena between the slider and the glass.²⁻⁶

Often, the exact flying height of a slider in an optical tester is also unknown to an adequate degree of precision. This limited degree of precision is due in part to variations in the optical properties of the slider material, including, most specifically, the real and the imaginary parts of the effective complex index of refraction. These quantities, commonly known as

the effective optical constants n and k , play an important role in calculating the absolute flying height. Traditionally, an ellipsometer measures the optical constants of a material, and the results are entered by hand into the flying-height test software. The ellipsometric geometry is very different from that of typical flying-height testers, so a completely separate instrument does the job.

The independent measurement of optical constants is a significant burden in optical flying-height testing. Furthermore, uncertainty in the values of n and k related to infrequent or incorrect ellipsometric analysis introduces systematic errors of several nanometers. These errors are often invisible to instrument qualification screens such as system-to-system correlation, repeatability, and reproducibility. Thus it is possible to have self-consistent flying-height data that is also consistently inaccurate.

Ideally, a flying-height tester should incorporate means to determine the optical constants *in situ* for every slider under test. To achieve this ideal, we propose a flying-height test geometry with an oblique angle of incidence and a high-speed homodyne interferometric receiver. The idea is to apply ellipsometry and radiometry directly to the flying-height problem, by treating the air gap as a dynamic thin film.⁷⁻⁹ We call our technique polarization interferometry, to distinguish it from the classical null ellipsometer with its rotating wave plates and polarizers. A significant benefit of polarization interferometry is that there is sufficient information to

P. de Groot is with Zygo Corporation, Laurel Brook Road, Middlefield, Connecticut 06455. A. Dergevorkian, T. Erickson, and R. Pavlat are with Zygo Flying High Test Division, 80A West Cochran Street, Simi Valley, California 93065.

Received 5 November 1997; revised manuscript received 31 March 1998.

0003-6935/98/225116-10\$15.00/0

© 1998 Optical Society of America

Table 1. Theoretical Zero-Spacing Error Δh Attributable to the Material Phase Change on Reflection of Al_2O_3 -TiC at Three Different Wavelengths

λ (nm)	n	k	Δh (nm)
405	2.15	0.55	8.8
633	2.14	0.47	12.1
830	2.13	0.61	20.1

solve for n and k as part of the flying-height test procedure. This paper describes how we calculate n and k and also provides an estimate of uncertainty and its effects on the final flying height.

2. Optical Constants of Sliders

Muranushi *et al.*¹⁰ were the first to describe in detail the importance of including the optical properties of slider materials in optical flying-height testing. The fundamental issue is the phase shift that occurs at the slider air-bearing surface (ABS) on reflection. In a conventional flying height tester there is no way to distinguish between a phase shift on reflection and the actual gap between the slider and the ABS. Muranushi *et al.*¹⁰ refer to this problem as a zero-spacing error (ZSE). As is shown in Table 1, the ZSE can be as large as 20 nm, which is the same magnitude as the flying height of modern high-performance sliders.¹¹ It is therefore critical to characterize and correct for the optical properties of the ABS.

The most common material for the body and ABS of read-write sliders is an amalgam of alumina (Al_2O_3) and titanium carbide (TiC). Under an optical microscope, the polished ABS shows grains of brightly reflecting TiC imbedded in alumina. The grains are typically a few micrometers wide, and a scanning-probe microscope reveals that the TiC is raised several nanometers above the alumina. A light beam incident on such a surface diffracts into a broad range of angles, with a resultant amplitude and phase that depends strongly on the size, distribution, and relative surface height of the TiC. The apparent reflectivity of such a surface depends, therefore, on the surface structure, the angle of incidence, and the numerical aperture of the imaging optics.

Given the material complexity of the ABS surface, it is not easy to predict its optical properties. It has become common practice in flying-height testing to model the complicated physical structure of Al_2O_3 -TiC as a smooth, homogeneous material for which it is possible to calculate the reflected electric field with a single, complex index of refraction. This simplified model assumes that the effective n and k measured by an ellipsometer are sufficient to estimate the complex reflectivity of the ABS for any optical system, including any material-dependent phase shifts.

Assuming that it is meaningful to define an effective n and k of the slider ABS, the complex reflectivity

Table 2. Intensity Reflectivity of Four Al_2O_3 -TiC Samples at a Wavelength of 633 nm Compared with the Theoretical Predictions with n and k

Ellipsometry		Reflectivity	
n	k	Theory	Measured
2.16	0.40	0.148	0.122
2.22	0.43	0.157	0.127
2.19	0.56	0.165	0.132
2.37	0.54	0.185	0.144

for s - and p -polarized light follows from the Fresnel equations¹²:

$$r_s' = \frac{\tan(\phi - \bar{\phi})}{\tan(\phi + \bar{\phi})}, \quad (1)$$

$$r_p' = -\frac{\sin(\phi - \bar{\phi})}{\sin(\phi + \bar{\phi})}. \quad (2)$$

Here ϕ is the angle of incidence and $\bar{\phi}$ is the (complex) angle of refraction. The angles are related by Snell's law:

$$\tilde{n} \sin(\bar{\phi}) = \sin(\phi), \quad (3)$$

where

$$\tilde{n} = n + ik \quad (4)$$

is the effective complex refractive index of refraction, found when conventional ellipsometry is performed.¹³ The Fresnel Eqs. (1) and (2) are the starting point for the theoretical estimates of ZSE presented in Table 1.

In reality, Eqs. (1) and (2) are only approximately true, because of the heterogeneous nature of the slider material. For example, it should be possible to calculate the intensity reflectivity at normal incidence by use of the formula

$$R = \left| \frac{\tilde{n} - 1}{\tilde{n} + 1} \right|^2. \quad (5)$$

This is an easy result to check experimentally; simply measure the incident and reflected intensities for a He-Ne laser beam. We have performed this experiment using the same laser and small-aperture collection optics for both 50° ellipsometry and normal-incidence reflectance measurements. The results in Table 2 for several different types of Al_2O_3 -TiC show that the calculated R with the effective n and k is consistently wrong by approximately 20%. This error indicates that the simple n and k model is not entirely satisfactory for heterogeneous materials such as Al_2O_3 -TiC. A detailed theoretical analysis also shows that the n and k model overestimates the ZSE by approximately 3 nm, over a wide range of Al_2O_3 -TiC compositions.¹⁴

Although there are clear deficiencies in the n and k model, the evidence suggests that this simplification is still useful and considerably better than ignoring

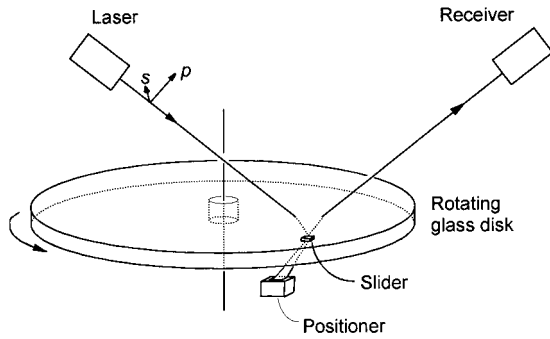


Fig. 1. Polarization interferometer for flying-height testing of magnetic read-write sliders. A rotating glass substrate takes the place of the magnetic disk to facilitate optical inspection of the gap. The receiver measures the polarization-dependent complex reflectivity of the slider-glass interface. The source is a 3-mW, 670-nm laser diode.

material effects altogether. The theory calculations in Table 2 have the wrong absolute magnitudes, but nonetheless properly rank the sample materials according to their relative reflectivities. There is also ample theoretical and experimental evidence to suggest that changes in the ZSE are well correlated to changes in the effective optical constants. For these reasons, Muranushi *et al.*¹⁰ proposed ellipsometric analysis as a means of characterizing slider materials for optical flying-height testing.¹⁰ Their approach has become accepted standard practice in the measurement procedures of commercial test equipment.¹⁵⁻¹⁷

Whatever the limitations of the n and k model, once we accept it as a useful and meaningful approximation, it makes sense to combine the role of the ellipsometer with that of the flying-height tester. This advance reduces the measurement errors attributable to infrequent or incorrect ellipsometric analysis. Consequently, one of our goals has been to develop an optical-sensing technology that measures the effective optical constants n and k of sliders during flying-height testing. As we shall show, we achieve this by analysis of the polarization state of light reflected from the slider-glass interface.

3. Polarization Interferometry

Figure 1 shows the basic optical geometry of our instrument, which is the outcome of several years of research beginning with the Sommargren's phase-shifting flying-height tester.¹⁸ The oblique incidence defines two orthogonal polarization components s and p , where p polarization is parallel to the plane of incidence. When the Jones calculus is used, the incident electric field is

$$E = \begin{pmatrix} E_s \\ E_p \end{pmatrix}. \quad (6)$$

For example, if the incident beam is linearly polarized with equal s and p components, then $E_s = E_p = 1/\sqrt{2}$. The electric-field components $E_{s,p}$ are complex numbers, so that any relative phase shift be-

tween the polarization components may be represented as a complex phase angle.

The combined reflections from the slider surface and the surface of the glass disk modify the polarization state of the beam. The electric field for the reflected beam is

$$E^r = SE, \quad (7)$$

where

$$S = \begin{bmatrix} z_s & 0 \\ 0 & z_p \end{bmatrix}, \quad (8)$$

and $z_{s,p}$ are the effective reflectivities of the slider-glass combination. The effective reflectivities are given by

$$z_{s,p}(\beta) = \frac{r_{s,p} + r_{s,p}'' \exp(i\beta)}{1 + r_{s,p}r_{s,p}'' \exp(i\beta)}, \quad (9)$$

where β is given by

$$\beta = 2kh \cos(\phi), \quad (10)$$

and the subscripts refer to the s - and the p -polarization states. The reflectivities $r_{s,p}$ are for the glass-air boundary, whereas the reflectivities $r_{s,p}''$ refer to the air-slider boundary. A constant, real parameter μ accounts for the difference between the n and k model and the reflective properties of typical slider materials:

$$r_{s,p}'' = (1 - \mu)r_{s,p}', \quad (11)$$

where $r_{s,p}'$ is the reflectivity calculated from the Fresnel formulas [Eqs. (1) and (2)].

Introducing the μ factor in Eq. (11) to account for scattered-light loss simplifies comparison with traditional ellipsometric determination of the effective n and k (see Table 2). The effect of μ on the calculated ZSE is small. Its only significant effect is to provide a better match between the predictions of the n and k model and the measured intensity reflectivity of the slider. We set the μ parameter to 0.05 (=10% intensity loss), which is a compromise between the measured value for heterogeneous Al_2O_3 -TiC and the theoretical value for true homogeneous materials.

The S matrix in Eq. (8) is a function of flying height; therefore the polarization state of the reflected electric field E^r can also be related to flying height. The homodyne interferometric receiver in Fig. 1 measures an intensity I and a phase θ and is defined by

$$I = |E_s^r|^2 + |E_p^r|^2, \quad (12)$$

$$\theta = \arg(E_s^r) - \arg(E_p^r). \quad (13)$$

In Fig. 2 a theoretical parametric I - θ curve of intensity and phase data is compared with experimental data.

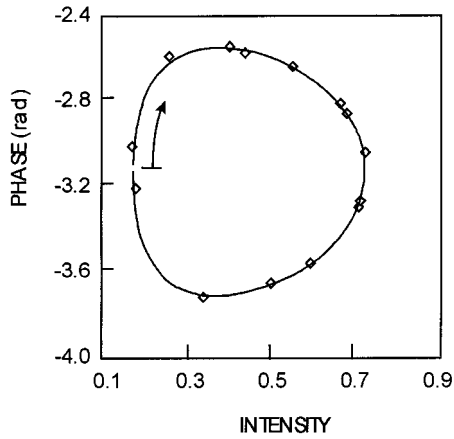


Fig. 2. Comparison of theoretical (solid circle) and experimental intensity and phase data. The arrow indicates the direction of increasing flying height, starting from contact. The experimental data were acquired (at several different locations on the ABS) by use of polarization interferometry of a read-write slider in steady flight.

4. Simultaneous Solution for n , k , and Flying Height

For every slider n and k value, there is a corresponding parametric I - θ curve. The key to determining n and k *in situ* is the realization that I - θ curves overlap at only two points, so that three or more I - θ values at different heights distinguish any given curve from all other possibilities.¹⁹ The idea therefore is to acquire data over a range of unknown heights, and find the n and k for the best possible match of experimental and theoretical I - θ values by use of a least-squares analysis. We refer to this process as calibration.

In defining a merit function for the least-squares analysis, it is useful to map the theoretical intensity and phase values I , θ into new variables Π and Ω defined by

$$\begin{aligned} I' &= I + 0.1, \\ \Omega &= -I' \sin(\theta), \\ \Pi &= -I' \cos(\theta). \end{aligned} \quad (14)$$

The Π - Ω variables have a quasi-sinusoidal, quadrature dependence on flying height, which results in a more linear system response than when the phase and the intensity are used directly. The choice of the 0.1 intensity offset optimizes this near-quadrature dependence for typical slider reflectivities.

Measured values of Π and Ω , denoted Π^m and Ω^m , require a measured intensity I^m that has been properly normalized according to the digitization range of the electronic analog-to-digital converter. The normalization strategy with the slider removed involves a background intensity measurement I_s^{bak} for the s -polarized light. Then

$$I^m = I_{\text{AD}}/I_0, \quad (15)$$

where I_{AD} is an intensity measured in analog-to-digital counts and the normalization constant is

$$I_0 = I_s^{\text{bak}}/R_s, \quad (16)$$

where R_s is the reflectivity of the bare glass.

The phase data do not require normalization, but they do require compensation for stress birefringence in the glass disk.^{20,21} Most often, stress caused by disk rotation introduces a constant offset in the phase data. One determines the offset with the slider removed by measuring this background phase shift introduced by the bare glass. In some measurement configurations, such as nonzero skew, two background phase measurements are necessary, but the basic concept is the same. For the purposes of this paper, we assume that the measured phase data have already been properly compensated.

The theoretical Π and Ω require values for n and k . Let us assume for the moment that we have chosen reasonable values for the optical constants and that we have acquired intensity and phase data over a range of N flying heights. The data analysis involves a multivariate chi-square function²²:

$$\hat{\chi}_i^2(h) = \frac{1}{2} \left\{ \left[\frac{\Pi_i^m - \Pi(h)}{\sigma_\Pi} \right]^2 + \left[\frac{\Omega_i^m - \Omega(h)}{\sigma_\Omega} \right]^2 \right\}, \quad (17)$$

where σ_Π and σ_Ω are the standard deviations for normally distributed noise in the measured values Π^m and Ω^m . The calculation of an individual flying height involves a search for the minimum value $\hat{\chi}_{\min}^2$, with the height h as the free parameter. When this process is completed for all flying heights, we can define a global merit function

$$M = \frac{1}{\nu} \sum_{i=0}^{N-1} (\hat{\chi}_{\min}^2)_i, \quad (18)$$

where $\nu = N - 2$ is the number of degrees of freedom. This global merit function characterizes the goodness of fit between the experimental and the theoretical data. The smaller the merit M , the better the fit.

A strategy for simultaneously solving for flying heights and an unknown n and k should now be evident: vary n and k in search of those values that provide the best global merit M . Solving for n and k involves an iterative search in two dimensions. Typically, two or three iterations for both optical constants will result in a stable convergence to the correct values. A critical aspect of this process is the availability of interference phase information, which makes it possible to draw parametric curves such as the one shown in Fig. 2. It is unlikely, for example, that meaningful n and k can be determined from intensity data alone.²³

5. Fit Quality and Uncertainty

The next logical question is how accurately a polarization interferometer can determine n , k , and flying height h . The iterative process for determining n and k is complete when the merit function M is as small as it can be. The minimum value of M is a

measure of the final agreement between experiment and theory, given realistic values for the standard deviations σ_{Π} and σ_{Ω} . This minimum value is therefore an indication of the quality of the fit, the accuracy of the theoretical model, and the uncertainty in the final measurement.

In flying-height test equipment, the most significant limitation on precision is unknown systematic measurement errors, as opposed to truly random noise. These errors include the nonlinear response of the optics and the electronics, as well as problems associated with dynamic system calibration with real sliders. Although errors of this kind do not strictly obey Gaussian statistics, they are still random in the sense that they are unpredictable and often unrepeatable. For example, the homodyne receiver in the polarization interferometer of Fig. 1 is composed of two Wollaston prisms, a quarter-wave plate and four photodetectors.²⁴ Error sources such as polarization mixing and other forms of coherent noise introduce uncertainty into the photodetector measurements. The variance of these errors tend to scale with the light intensity. The intensity is itself a function of the flying height of the slider, with the consequence that the measurement errors are also height dependent.

The observations of the previous paragraph translate into an estimate of the normalized variance σ_I^2 for the total intensity I given by

$$\sigma_I^2 = I'\sigma^2, \quad (19)$$

where σ is a constant. The same error sources propagate through the phase-measurement algorithms,²⁵ resulting in phase with a variance of approximately

$$\sigma_{\theta}^2 = \sigma^2/I'. \quad (20)$$

The phase and the intensity variances transform to the Π - Ω parameters as follows:

$$\begin{aligned} \sigma_{\Omega}^2 &= \sigma_{\theta}^2 \Pi^2 + (\sigma_I/I')^2 \Omega^2, \\ \sigma_{\Pi}^2 &= \sigma_{\theta}^2 \Omega^2 + (\sigma_I/I')^2 \Pi^2. \end{aligned} \quad (21)$$

Noting that the sum of the squares of Π and Ω is I'^2 , we can now show that

$$\sigma_{\Omega}^2 = \sigma_{\Pi}^2 = I'\sigma^2. \quad (22)$$

We emphasize that this error analysis is meant to be physically reasonable, not rigorous. However, Eq. (22) does lead to a very convenient conclusion: The Π and Ω variables in the least-squares calculation have equal weight for all flying heights. We need only specify one constant value σ to normalize the chi-square function in Eq. (17) properly.

When Eq. (22) is used, the merit function in Eq. (18) simplifies to

$$M = \frac{1}{\nu\sigma^2} \sum_{i=0}^{N-1} (\chi_{\min}^2)_i, \quad (23)$$

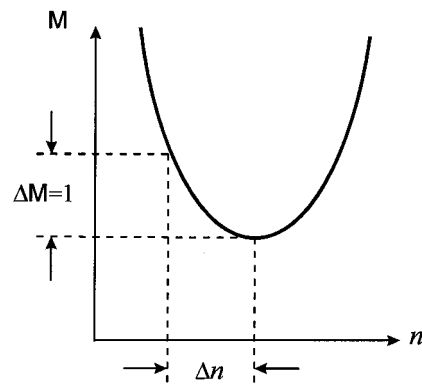


Fig. 3. Calculation of the uncertainty Δn with the sensitivity of the merit function M to variations in n .

where

$$\chi_i^2(h) = \frac{[\Pi_i^m - \Pi(h)]^2 + [\Omega_i^m - \Omega(h)]^2}{2I'(h)}. \quad (24)$$

Armed with this normalized merit function M , we are now in a position to estimate the uncertainties Δn and Δk and their effect on the overall system accuracy. Figure 3 illustrates the procedure for determining Δn . After determining the optical constants n and k that minimize M , we find the change Δn that changes M by one, assuming that we allow freedom in the k value to reoptimize M . The change Δn is the one-sigma uncertainty in n . Thus if the merit M is only weakly dependent on the index n or if the σ is very large, the resultant uncertainty will be higher.

The procedures for calculating Δn and Δk require a good estimate of the measurement uncertainty σ . Analysis of known error sources, such as the nonlinear response of the homodyne receiver, fluctuations in laser power, and uncompensated photoelastic stress in the glass disk, provide an estimate of $\sigma = 0.005$. This is equivalent to a typical uncertainty of 20 mrad P-V for the phase and 2% mrad P-V for the intensity. With this value of σ , a numerical analysis for a slider under realistic conditions yields an uncertainty $\Delta n = \Delta k = 0.04$.²⁶ This result compares favorably with the uncertainty in standard ellipsometry for Al_2O_3 -TiC materials.

So how do the uncertainties in the n and k calibration couple into uncertainty in flying height? To answer this question, we first change the n value by Δn and calculate the height change Δh_n caused by this change in n . Then we do the same for k to get an uncertainty Δh_k . The square root of the average variances is the net rms uncertainty in flying height:

$$\Delta h = \left[\frac{1}{2} (\Delta h_n^2 + \Delta h_k^2) \right]^{1/2}. \quad (25)$$

This procedure can be done for every measurement point. Figure 4 shows the results of a numerical analysis in which this equation is used to determine the final flying-height uncertainty as a function of flying height. This result confirms that polarization

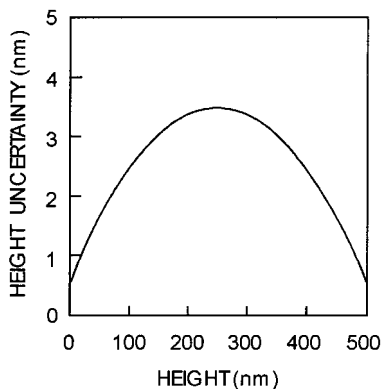


Fig. 4. Theoretical estimate of flying-height errors in polarization interferometry. These data correspond to a rms uncertainty in both n and k of 0.04.

interferometry provides satisfactory results over the entire height range, while it simultaneously provides the appropriate values of n and k for the test slider. The performance is particularly good at low flying heights, where correct values of n and k have the greatest influence on relative accuracy.

6. Calibration Techniques

Reliable n and k calibration requires several intensity and phase measurements over a range of flying heights. As Fig. 5 shows, the larger the height range for calibration, the more accurate and repeatable the n and k . The minimum required calibration height range H for a given uncertainty in n and k varies considerably with the lowest height within the range. The curve in Fig. 6 shows the range H to maintain an uncertainty in n and k below 0.05.

A well-known calibration technique for flying-height testers involves removing or unloading the slider from the disk and loading it back again to generate a time-dependent range of flying heights. A high-speed sensor (250 kHz) is needed to follow the

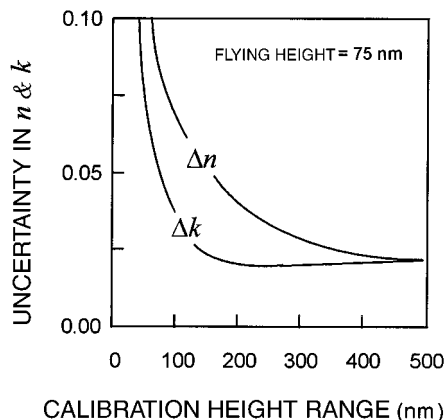


Fig. 5. Uncertainty in n and k as a function of the calibration height range. The calculation assumes phase and intensity measurements over a range of evenly spaced flying heights, with the lowest flying height at 75 nm. The calibration height range is the difference between the highest and the lowest flying height.

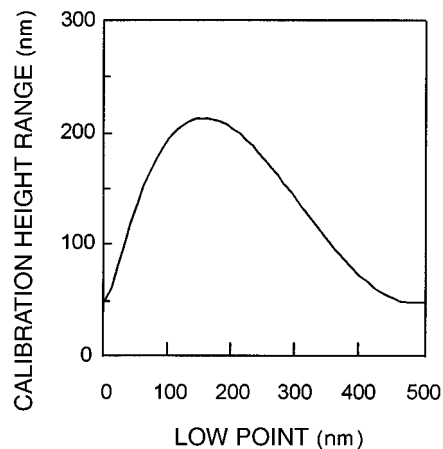


Fig. 6. Minimum calibration range to maintain a rms uncertainty for n and k below 0.05.

highly dynamic motion of the slider. This procedure, sometimes called a retract calibration, is common in traditional flying-height testers that use intensity data alone. With polarization interferometry, retract calibration is most useful for verifying n and k at specific points on the ABS. Examples of phase and intensity data for a retract calibration appear in Ref. 27. If high-quality retract calibration is available over a large height range, it is even possible to solve directly for n and k with analytical formulas in place of a least-squares analysis.⁷

Although a mechanical retract of the slider is still the most common technique for calibrating flying-height testers, the dynamical properties of several new slider designs are not consistent with this practice. For these modern sliders, the quality of the retract data is insufficient for accurate calibration.²⁸ Further, repeated loading and unloading of the slider assembly can damage the sample.

Polarization interferometry provides an attractive alternative to the traditional retract calibration. As is evident from Fig. 6, the required range H for calibration is usually small enough that it is practical for one to calibrate it by scanning to multiple locations on the slider ABS. The majority of sliders in common use today are pitched slightly from trailing to leading edge in normal flight, typically providing greater than 50 nm of height variation. This is an insufficient range for calibration of traditional three-wavelength ($3-\lambda$) intensity testers, which require min-max information so as to scale the experimental data properly.²⁹ However, as Fig. 7 shows, calibration by ABS scanning becomes progressively easier for polarization interferometry as flying heights decrease.

The simplest form of ABS scanning is a sequence of measurements at discrete positions, as shown in Fig. 8. With appropriate encoding hardware to record the exact measurement locations, the data acquisition takes the form of a rapid, continuous scan of the ABS. With continuous scanning, it is possible to acquire data for hundreds of ABS locations in a few

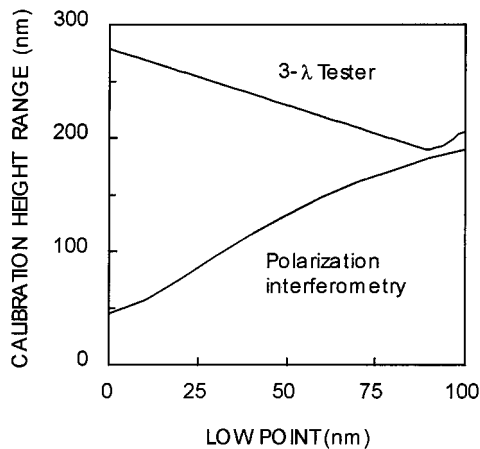


Fig. 7. Comparison of the minimum calibration range for a 3- λ intensity tester (upper curve) with that of a polarization interferometer (lower curve). The 3- λ curve is the minimum range needed to normalize experimental intensity data at 436-, 548-, and 580-nm wavelengths. As flying heights decrease, it becomes increasingly attractive to use polarization interferometry because of its relative ease of calibration.

seconds. The resulting high-density data provides detailed, noise-resistant information regarding the ABS profile. A second-order surface fit to experimental data is illustrated in Fig. 9, showing the typical curvature or crown of the ABS. The ability to calibrate the instrument without a mechanical retract of the slider is a significant and fundamental advantage of polarization interferometry.

A reasonable alternative approach to acquiring large amounts of data is to employ one or more CCD cameras.³⁰⁻³² The advantage of such a system is that multiple ABS locations are accessed simultaneously, without the need for mechanical scanning. Lacey and Durán³³ describe an interesting CCD-

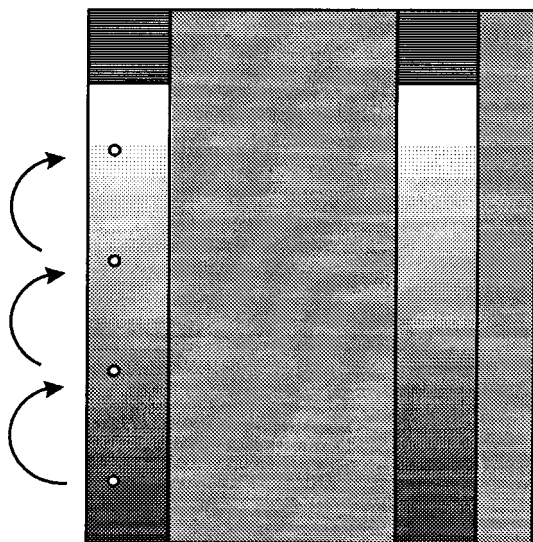


Fig. 8. Data acquisition by use of ABS scanning. The single-point measurement beam moves from point to point on the ABS, acquiring data at different heights for the n and k calibration.

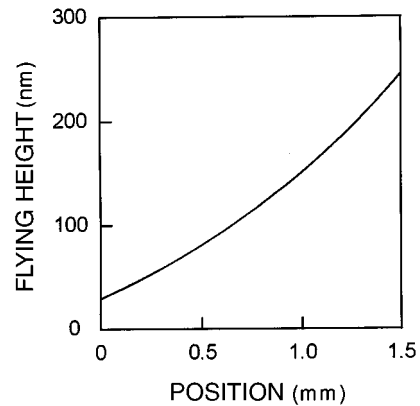


Fig. 9. Cross section of a cylindrical surface fit of height data obtained when the slider ABS is scanned as shown in Fig. 8. The obvious curvature is referred to as the ABS crown and is generated by polishing the slider on a spherical lap. The surface fit permits extrapolation to the read-write element of the slider.

based ellipsometric system that may have useful applications in the future.

7. Experimental Verification

We have verified n and k calibration principle in both laboratory tests with well-characterized samples and in final performance tests with Al_2O_3 -TiC read-write sliders.

Laboratory tests have been extensive, and they verify both the repeatability and the absolute accuracy of polarization interferometry. In these tests the sensor is arranged so as to scan laterally across a gap standard composed of a silicon-carbide (SiC) flat and a slightly domed glass window (Fig. 10).³⁴ The glass is placed in contact with the highly polished SiC, and the 20-m convex radius of the glass provides a stable range of gaps for calibration.³⁵ Figure 11 shows a typical scan of the gap standard by use of polarization interferometry. The extended contact region, known historically as Newton's black spot, is an excellent means of verifying correction for ZSE.

Because the optical sensor is part of a manufactured instrument product, we have been able to perform a very strenuous laboratory test of the accuracy and the repeatability of our n and k technique. We measured the same test sample with 16 different sensors taken from the production line, over a period

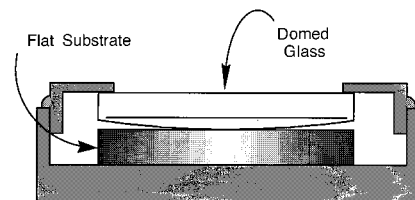


Fig. 10. Gap standard for verifying the accuracy of polarization interferometry. The glass has a 20-m radius of curvature, and when placed in contact with the flat SiC substrate, provides a well-controlled range of gaps. The contact region is a small circular area of low reflectivity.

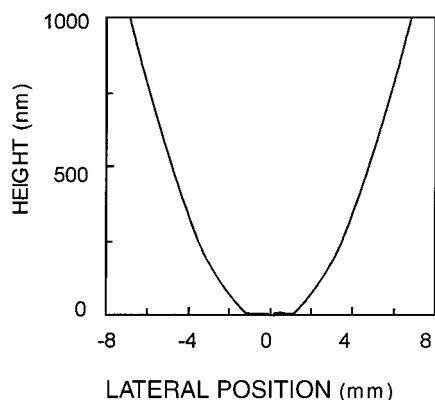


Fig. 11. Polarization interferometry data for the gap standard shown in Fig. 10 with a SiC substrate. The contact region between -1 and $+1$ mm has an average measured gap of 0.5 nm. The increasing heights to either side of the contact region are caused by the 20 -m radius of curvature of the glass.

of several months. The results in Table 3 show standard deviations for n and k that are both very close to the prediction of 0.04 , which appears in Section 5. This is a test not only of the measurement uncertainty but also of the reproducibility of the manufacturing process. The averaged values of n and k also correlate to within 0.05 to conventional null ellipsometry at the same 670 -nm wavelength. The average measured contact height is 1.3 nm with a standard deviation of 0.65 nm, which is in excellent agreement with Fig. 4.

The n and k calibration is also highly repeatable in dynamic testing with actual sliders. Table 4 shows the measured n and k for the two rails of an Al_2O_3 -TiC catamaran slider by use of ABS scanning. The disk spin speed for was 5000 rpm, and the pitch height was 230 nm. After each trial, the slider was unloaded from the disk, reloaded, and repositioned for the next trial. The rms repeatability for this test, which uses the same sensor and the same part, is better than 0.002 for both n and k .

Table 3. Experimental Determination of the Optical Constants of SiC at a Wavelength of 670 nm by Polarization Interferometry with 16 Different Sensors^a

Trial	n	k	Trial	n	k
1	2.61	0.06	9	2.60	0.04
2	2.53	0.04	10	2.54	0.05
3	2.49	0.05	11	2.52	0.02
4	2.66	0.06	12	2.48	0.03
5	2.56	0.01	13	2.49	0.05
6	2.62	0.03	14	2.63	0.12
7	2.57	0.03	15	2.66	0.06
8	2.61	0.06	16	2.66	0.07
			n	k	
Standard deviation			0.06	0.03	
Average values			2.58	0.05	
Independent ellipsometer			2.63	0.09	

^aOver a period of several months.

Table 4. Dynamic Repeatability of Calibration for an Al_2O_3 -TiC Slider with ABS Scanning

Inner Rail		Outer Rail	
n	k	n	k
2.2273	0.6000	2.2300	0.6076
2.2273	0.6000	2.2317	0.6048
2.2280	0.6019	2.2327	0.6059
2.2292	0.6012	2.2311	0.6049
2.2282	0.5999	2.2308	0.6057
2.2279	0.5999	2.2299	0.6041
2.2266	0.5979	2.2285	0.6006
2.2262	0.5964	2.2295	0.6016

Extensive testing in manufacturing and at customer facilities indicates that a realistic expectation for agreement between polarization interferometry and independent ellipsometry of Al_2O_3 -TiC is ± 0.1 for both n and k . We would like to see tighter and more consistent correlation, but this goal has remained elusive. The limits to correlation when one uses Al_2O_3 -TiC materials are rooted in the n and k approximation, which, as we have noted in Section 2, does not correctly predict the intensity reflectivity. Because our flying-height tester calibrates for the apparent intensity reflectivity directly, the effective n and k for polarization interferometry can differ from ellipsometric measurements.

A more direct means of verifying that the sensor is properly calibrated for material properties is to place a bulk sample of Al_2O_3 -TiC into the gap standard shown in Fig. 10. The curve in Fig. 12 represents typical results for the contact region between the glass and an Al_2O_3 -TiC sample coated with a 2 -nm SiO_2 adhesion layer and a 6 -nm diamondlike carbon. The 1 -nm average surface height within the contact region indicates that the n and the k calibration values of 2.13 and 0.30 , respectively, are properly compensating for ZSE.

We observe a greater variation in average contact height from sample to sample with Al_2O_3 -TiC than

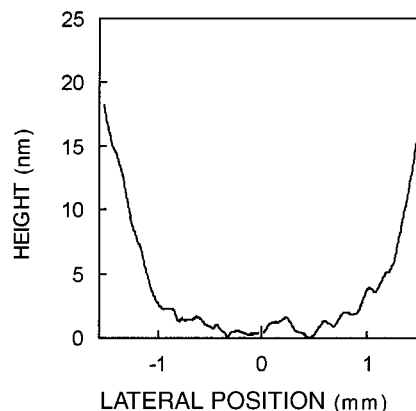


Fig. 12. Contact region of the gap standard shown in Fig. 10 for a flat substrate made of carbon-coated Al_2O_3 -TiC. For this sample of common slider material, the *in situ* n and k analysis reduces the ZSE to less than 1 nm.

we do with SiC. We attribute this variation in part to the 2-nm rms surface roughness of this material, which results in approximately the same rms range of contact heights. The surface roughness is also responsible for a persistent ambiguity in the definition of flying height for real sliders. It appears that the measured flying height corresponds most directly to the average height of the raised TiC grains within the Al₂O₃-TiC, because of a small but constant overestimate of the ZSE when an effective n and k are used.¹⁴ This small offset compensates for surface roughness and actually improves correlation between optical measurements and contact test, such as are shown in Fig. 12.

8. Summary and Conclusions

Our research shows that it is possible and practical to measure the optical constants of every slider during optical flying-height testing, thus obviating the need for a separate metrology step with an ellipsometer.³⁶ For achieving this goal, our instrument measures the polarization-dependent variation in the reflectivity of the slider-glass interface, with light incident at an oblique angle (Fig. 1). The same instrument can then perform the flying-height measurement and simultaneously determine the effective n and k . This capability increases confidence in the final result, especially at low flying heights.

The n and k calibration consists of a least-squares fit of theoretical intensity and phase curves to experimental data acquired over a range of flying heights (Fig. 2). One may acquire the data for calibration either by retracting the slider or by scanning the slider ABS. The ability to calibrate by ABS scanning is particularly attractive with modern negative-pressure sliders.

Assuming typical and reasonable levels of uncertainty for phase and intensity data, we predict a typical rms uncertainty for n and k of 0.04 (Fig. 5). Experimental research confirms this numerical value (Table 3). This uncertainty in n and k calibration propagates to a typical 2-nm uncertainty in flying height, progressing to less than 1 nm near contact. Experiments with a gap standard (Figs. 10 and 11) confirm this prediction.

Further improvements will arrive from an improved understanding of the optical properties of common slider materials. We would also like to see a better definition of the meaning of flying height, and particularly of contact, for sliders having a surface roughness of several nanometers. These improvements require, at a minimum, an optical technology capable of detailed polarization analysis. We believe that our instrument is a significant step forward in the development of this technology.

The polarization interferometer is the product of L. Deck, J. Soobitsky, and J. Biegen working together with the authors of this paper. The integrated system, including spin stand, software, and parts handling, is the product of several years of dedicated effort by the Zygo Flying Height Division in Califor-

nia. Leonard Research Corporation provided independent ellipsometric analysis to demonstrate n and k correlation. Finally, the authors acknowledge the contributions of J. Morace and R. Gecewicz in handling manufacturing issues and the efforts of all those who have worked to make this instrument a successful commercial product.

References and Notes

1. B. Bhushan, *Tribology and Mechanics of Magnetic Storage Devices* (Springer-Verlag, New York, 1990) pp. 765–797.
2. W. Stone, "A proposed method for solving some problems in lubrication," *The Commonwealth Engineer* (1 November 1921), pp. 115–122.
3. J. M. Fleischer and C. Lin, "Infrared laser interferometer for measuring air-bearing separation," *IBM J. Res. Develop.* **18**, 529–533 (1974).
4. T. Ohkubo and J. Kishigami, "Accurate measurement of gas-lubricated slider bearing separation using laser interferometry," *Trans. ASME* **110**, 148–155 (1988).
5. C. Lacey, J. A. Adams, E. W. Ross, and A. Cormier, "A new method for measuring flying height dynamically," *Proceedings of DiskCon '92* (International Disk Drive Equipment and Materials Association, Sunnyvale, Calif., 1992), pp. 27–42.
6. T. E. Erickson and J. P. Lauer, "Multiplexed laser interferometer for non-dispersed spectrum detection in a dynamic flying height tester," U.S. patent 5,673,110 (30 September 1997).
7. P. de Groot, L. Deck, J. Soobitsky, and J. Biegen, "Polarization interferometer for measuring the flying height of magnetic read-write heads," *Opt. Lett.* **21**, 441–443 (1996).
8. P. de Groot, J. Biegen, L. Deck, A. Dergevorkian, T. Erickson, J. Morace, R. Pavlat, and J. Soobitsky, "Polarization interferometer for flying height testing," in *Proceedings of Future Dimensions in Storage Symposium* (International Disk Drive Equipment and Materials Association, Sunnyvale, Calif., 1997), pp. 89–94.
9. P. de Groot, "Optical gap measuring apparatus and method," U.S. patent 5,557,399 (17 September 1996).
10. F. Muranushi, K. Tanaka, and Y. Takeuchi, "Estimation of zero-spacing error due to a phase shift of reflected light in measuring a magnetic head slider's flying height by light interference," *Adv. Info. Storage Syst.* **4**, 371–379 (1992). The same paper was presented at the ASME Winter Annual Meeting, Atlanta, Ga., 1991.
11. The calculations for Table 1 also appear in the paper "Interferometric measurement of disk/slider spacing: the effect of phase shift on reflection," by C. Lacey, R. Shelor, A. Cormier, and R. E. Talke, *IEEE Trans. Magn.* **MAG-29**, 3906–3910 (1993).
12. M. Born and E. Wolf, *Principles of Optics* (Pergamon, New York) p. 40.
13. Following Born and Wolf, we prefer to use the $n + ik$ definition of the complex index, rather than the more common $n - ik$.
14. P. de Groot, "Optical properties of alumina titanium carbide sliders used in rigid disk drives," (submitted to *Appl. Opt.*).
15. R. Pavlat, "Flying height measurement systems and slider absorption," *IDEMA Insight* **7**, 1 (1994).
16. Y. Li, "Flying height measurement on Al₂O₃ film of a magnetic slider," presented at the *American Society of Mechanical Engineers Tribology Conference*, paper 96-TRIB-61 (San Francisco, Calif., 13–17 October 1996).
17. K. Lue, C. Lacey, and F. E. Talke, "Measurement of flying height with carbon overcoated sliders," *IEEE Trans. Magn.* **30**, 4167–4169 (1994).
18. G. Sommargren, "Flying height and topography measuring interferometer," U.S. patent 5,218,424 (8 June 1993).
19. Generally, it is not possible to calculate a film thickness as well

- as the optical constants from a single ellipsometric measurement; hence the need for three or more flying heights for proper n and k calibration. See, for example, R. M. A. Azzam and N. M. Bashara, *Ellipsometry and Polarized Light* (Elsevier, Amsterdam, 1987), p. 317.
20. P. de Groot, "Birefringence in rapidly-rotating glass disks," *J. Opt. Soc. Am. A* **15**, 1202–1211 (1998).
 21. P. de Groot, "Method and apparatus for measuring and compensating birefringence in rotating disks," U.S. patent 5,644,562 (1 July 1997).
 22. W. H. Press, S. A. Teukolsky, W. T. Vetterling, and B. P. Flannery, *Numerical Recipes in C*, 2nd ed. (Cambridge U. Press, Cambridge, UK, 1992) p. 680.
 23. Not everyone agrees that interference phase information is essential for n and k . K. H. Womack and A. Butler have proposed to calculate the two parameters n and k using only the intensity reflectivity at normal incidence, together with off-site characterization of the material. Their paper, entitled "In-situ n & k phase compensation in an interferometric flying height tester," is available from Phase Metrics Corporation, 10260 Sorrento Valley Road, San Diego, Calif. 92121.
 24. P. de Groot, "Homodyne interferometric receiver and calibration method having improved accuracy and functionality," U.S. patent 5,663,793 (2 September 1997).
 25. C. P. Brophy, "Effect of intensity error correlation on the computed phase of phase-shifting interferometry," *J. Opt. Soc. Am. A* **7**, 537–541 (1990).
 26. Another way to express the uncertainty in the optical constants would be to calculate the ratios $\Delta k/k$ and $\Delta n/n$. However, this would create the misleading impression that the uncertainty improves for larger values of n and k . It would also create the false impression that measurement of k on a dielectric has an undefined uncertainty because the k is zero.
 27. P. de Groot, L. Deck, J. Soobitsky, and J. Biegen, "Optical flying-height testing of magnetic read-write heads," in *Lasers, Optics, and Vision for Productivity in Manufacturing I*, C. Gorecki, ed., Proc. SPIE **2782**, 47–57 (1996).
 28. C. Lacey, C. Durán, K. Womack, and R. Simmons, "Optical measurement of flying height," in *Proceedings of Future Dimensions in Storage Symposium* (International Disk Drive Equipment and Materials Association, San Diego, 1997), pp. 81–88.
 29. C. A. Durán, "Error analysis of a multiwavelength dynamic flying height tester," *IEEE Trans. Magn.* **32**, 3720–3723 (1996).
 30. R. B. Edwards, "Three-color laser interferometer," *IBM Technical Disclosure Bulletin* **16**, 595–596 (1973).
 31. T. Fukuzawa, T. Hisano, T. Morita, and K. Ikarugi, "Method and apparatus for measuring the flying height of a magnetic head above a disk surface at three wavelengths," U.S. patent 5,502,565 (26 March 1996).
 32. G. Sommargren, "Distance measuring interferometer and method of use," U.S. patent 4,606,638 (19 August 1986).
 33. C. Lacey and C. Duran, "Full surface detection of flying height with in-situ n & k measurement," *IDEMA Insight*, **9(6)**, 1, 9 (1996).
 34. P. de Groot, J. Biegen, L. Deck, and R. Smythe, "Calibration standard for optical gap measuring tools," U.S. patent 5,724,134 (3 March 1998).
 35. A similar arrangement for establishing known gaps for calibration appears in U.S. patent 5,220,408 to M. Mager, entitled "Method and apparatus for calibration of optical flying-height testers" (15 June 1993).
 36. Our technique does require an estimated value for the scattered light loss, in the form of the μ factor. However, the effect of an incorrect μ on the ZSE is small. It serves primarily to simplify comparison of our technique with traditional ellipsometry.